Assessment of an Eulerian atomization model on Diesel spray CFD simulations

J.M. García-Oliver, J.M. Pastor*, A. Pandal
CMT-Motores Térmicos, Universitat Politècnica de València, Spain
jgarciao@mot.upv.es, jopasen@mot.upv.es, adpanbla@mot.upv.es

N. Trask, D. P. Schmidt
Department of Mechanical and Industrial Engineering, University of Massachusetts, Amherst, USA
nat.trask@gmail.com, schmidt@acad.umass.edu

Abstract

This work presents an implementation and evaluation of the Σ-Y atomization model for Diesel spray CFD simulations. The Σ-Y model, originally proposed by Vallet and Borghi, is based on an Eulerian representation of the spray atomization and dispersion by means of a single-fluid variable density turbulent flow within a RANS framework. A finite-volume solver for model equations has been written using the OpenFOAM CFD open-source C++ library. Model predictions have been compared to experimental data from free Diesel sprays under non-vaporizing conditions. High-speed imaging and PDPA measurements have been used in order to evaluate model predictions. The model set-up study indicates that accurate predictions of spray penetration, as well as axial and radial velocity profiles, can be simultaneously achieved. Further parametric studies indicate that the Σ-Y model approach remains valid for a wide range of injection pressure and ambient density conditions typical of Diesel engine operation. Model accuracy is worse for low ambient density and injection pressure conditions. It is proposed that under these particular conditions, the slip between phases becomes more significant and the single velocity field assumption is less appropriate.

Introduction

The fuel injection process and subsequent fuel-air mixing formation play a major role in combustion and pollutant formation in Diesel engines. Therefore, an accurate prediction of these processes is required in order to produce reliable engine performance and emissions predictions. Diesel spray modelling is still a challenging task due to the complex interrelated phenomena involved; some of them, such as primary atomization or nozzle cavitation, are not fully understood.

The discrete droplet method (DDM) [1] has been widely employed for Diesel spray modeling on practical design applications for more than thirty years. This method applies a Lagrangian description for the liquid spray, which presents some well known drawbacks for dense two-phase flow modeling. Some basic hypotheses, such as low liquid volume fraction or homogeneously distributed parcels in the computational cells, are not valid in the near nozzle flow of Diesel sprays. In order to assure numerical stability and reasonable computational cost, it is often necessary to use grid sizes larger than the orifice diameter and then flow structures are not adequately resolved [2][3]. Moreover, the validity of isolated drop based models in this region with strong interaction between phases is hardly justified. Those issues usually require a 'best-practice' approach when using this method [4][5].

The so-called Σ-Y atomization model, initially proposed by Vallet and Borghi [6], has emerged as an alternative to the DDM for Diesel spray simulations [7][8][9][10][11]. This model is based in an Eulerian approach, which is more suitable for the description of the primary atomization occurring at the near field of Diesel sprays. The extent of the atomization process is computed from an interface surface density equation, and then it is not required to presume any particular shape for liquid fragments. Furthermore, this is a natural approach for including nozzle geometry flow effects on spray calculations [12]

In this work, an implementation of the Σ-Y model within the OpenFOAM [13] CFD framework is presented. The aim of the paper is to evaluate its application to Diesel spray modelling by comparing with experimental data. Those data were obtained on specific rigs for spray characterization, including both global and local parameters, such as tip penetration and droplet velocity, on a wide range of ambient and injection conditions.

* Corresponding author: jopasen@mot.upv.es

Model description

The Σ-Y model treats the liquid/gas mixture as a pseudo-fluid with a single velocity field. Under the assumption that the flow exiting the injector is operating at large Reynolds and Weber numbers, it is possible to assume a separation of the large scale flow features such as mass transport from the atomization process occurring at smaller scales. This allows the direct simulation of the large scale bulk transport of the liquid while unresolved turbulent transport is modelled using standard closures such as those used in Reynolds-averaged turbulence models.

To track the dispersion of the liquid phase an indicator function is used, taking a value of unity in the liquid phase and zero in the gas phase. The mean liquid volume fraction is denoted $\bar{Y}$ and the mean mass averaged fraction is defined as $\tilde{Y} = \frac{\overline{\rho Y}}{\bar{\rho}}$. The transport equation for the liquid mass fraction is then given by

$$\frac{\partial \bar{\rho}\tilde{Y}}{\partial t} + \frac{\partial \bar{\rho}\tilde{u}_i\tilde{Y}}{\partial x_i} = -\frac{\partial \bar{\rho}\overline{u_i'Y'}}{\partial x_i} \tag{1}$$

where u' denotes the density weighted turbulent fluctuations in velocity and Y' denotes turbulent fluctuations in volume fraction. The turbulent diffusion liquid flux captures the effect of the relative velocity between the two phases. While the approach used here assumes that the resolved momentum of the liquid/gas mixtures can be characterized by a single bulk velocity, the slip velocity can be defined as [14]

$$u_i\big|_l - u_i\big|_g = \frac{1}{\tilde{Y}\left(1-\tilde{Y}\right)} \cdot \overline{u_i'Y'} \tag{2}$$

Under the assumption that the two phases form an immiscible mixture, the mass-averaged value of the indicator function is related to the density by

$$\frac{1}{\bar{\rho}} = \frac{\tilde{Y}}{\rho_l} + \frac{1-\tilde{Y}}{\rho_g} \tag{3}$$

An equation of state is then assigned to each phase. The gas phase obeys an ideal gas law, while the liquid phase is treated with a linear compressibility ψ_l

$$\rho_g = \frac{p}{R_g T} \tag{4}$$

$$\rho_l = \rho_{l,o} + \psi_l\left(p - p_o\right) \tag{5}$$

where $\rho_{l,o}$ and p_o denote reference density and pressures, respectively, about which the equation of state is linearized. To finally close the above system of equations the temperature is obtained from a bulk mixture enthalpy equation and closures must be given for the terms resulting from Reynolds averaging. The closure in the liquid mass transport equation is assigned using a standard turbulent gradient flux model

$$\bar{\rho}\overline{u_i'Y'} = \frac{\mu_t}{Sc}\frac{\partial \tilde{Y}}{\partial x_i} \tag{6}$$

and the closure corresponding to the Reynolds stresses in the momentum equation is given by a modified *k-ε* model that accounts for the additional production caused by density fluctuations

$$\frac{\partial \bar{\rho}\tilde{k}}{\partial t} + \frac{\partial \bar{\rho}\tilde{u}_i\tilde{k}}{\partial x_i} = \frac{\partial}{\partial x_i}\left(\frac{\mu_t}{P_{rk}}\frac{\partial \tilde{k}}{\partial x_i}\right) - \bar{\rho}R_{ij}\frac{\partial \tilde{u}_j}{\partial x_i} - \overline{u_i'}\frac{\partial \bar{p}}{\partial x_i} - \bar{\rho}\tilde{\varepsilon} \tag{7}$$

$$\frac{\partial \bar{\rho}\tilde{\varepsilon}}{\partial t} + \frac{\partial \bar{\rho}\tilde{u}_i\tilde{\varepsilon}}{\partial x_i} = \frac{\partial}{\partial x_i}\left(\frac{\mu_t}{P_{r\varepsilon}}\frac{\partial \tilde{\varepsilon}}{\partial x_i}\right) + C_{\varepsilon 1}\frac{\tilde{\varepsilon}}{\tilde{k}}\left(-\bar{\rho}R_{ij}\frac{\partial \tilde{u}_j}{\partial x_j} - \overline{u_i'}\frac{\partial \bar{p}}{\partial x_i}\right) - C_{\varepsilon 2}\bar{\rho}\frac{\tilde{\varepsilon}^2}{\tilde{k}} \tag{8}$$

$$-\bar{\rho}\overline{u_i''u_j''} = \mu_t\left(\frac{\partial \tilde{u}_i}{\partial x_j} + \frac{\partial \tilde{u}_j}{\partial x_i} - \frac{2}{3}\frac{\partial \tilde{u}_l}{\partial x_l}\delta_{ij}\right) - \frac{2}{3}\bar{\rho}\tilde{k}\delta_{ij} \tag{9}$$

The averaged velocity fluctuations in Eqs. (7) and (8) is obtained as following [7],

$$\overline{u_i'} = \bar{\rho}\overline{u_i'Y'}\left(\frac{1}{\rho_l} - \frac{1}{\rho_g}\right) \tag{10}$$

The solution of the above equations fully characterizes the large-scale bulk motion of the flow. Several other options exist for obtaining closure in the above system of equations (see for example the discussion in [14] and [15]).

The small scale atomization is modelled by solving a transport equation for the evolution of the density of interphase surface area Σ originally proposed by Vallet and Borghi [6]. The evolution equation is given by

$$\frac{\partial \widetilde{\Sigma}}{\partial t}+\frac{\partial \tilde{u}_j \widetilde{\Sigma}}{\partial x_j}=\frac{\partial}{\partial x_j}\left(D_\Sigma \frac{\partial \widetilde{\Sigma}}{\partial x_j}\right)+(A+a)\widetilde{\Sigma}-V_s\widetilde{\Sigma}^2 \tag{11}$$

where D_Σ is a suitable diffusion coefficient usually taken as the turbulent viscosity ν_t over a Schmidt number. The terms A and a are inverse times scales that define the rate at which surface area is produced. Specifically, the A term models the creation of surface area via the stretching of the interface by mean velocity gradients. Vallet's original model takes this term to be proportional to the same time scale as that used in the production of kinetic energy in the traditional k-epsilon model.

$$A=\alpha_0 \frac{\overline{\rho u_i'' u_j''}}{\bar{\rho} k}\frac{\partial \tilde{u}_i}{\partial x_j} \tag{12}$$

The a term accounts for small-scale interface area production. Here there are several possibilities, but if it is assumed that the dominant mechanism is related to the collision and breakup of droplets, the inverse of droplet collision time scale may be used [7].

$$a_{coll}=\frac{\alpha_1}{(36\pi)^{2/9}}(l_t\Sigma)^{2/3}\left(\frac{\rho_l}{\bar{\rho}\tilde{Y}}\right)^{4/9}\frac{\varepsilon}{k} \tag{13}$$

Finally, the V_s term captures the effects of interface destruction by coalescence. It is determined by solving for the value of V_s that will provide an equilibrium value of Σ_{eq} set by a predicted equilibrium droplet radius.

$$\Sigma_{eq}=\frac{\tau_{prod}}{\tau_{destr}}=\frac{3\bar{\rho}\tilde{Y}}{\rho_l r_{eq}} \tag{14}$$

Upon selection of a suitable r_{eq}, the V_s, term is therefore given by

$$V_s=\frac{a_{coll}\rho_l r_{eq}}{3\bar{\rho}\tilde{Y}} \tag{15}$$

To fix the equilibrium radius, there are, again, several options but as in Vallet et al.[7] it is finally given by

$$r_{eq}=\alpha_2\frac{\sigma^{3/5}l_t^{2/5}}{k^{3/5}}\frac{(\bar{\rho}\tilde{Y})^{2/15}}{\rho_l^{11/15}} \tag{16}$$

Together with the mass averaged volume fraction, the interface surface area density can be used to calculate the local Sauter mean diameter of the spray.

$$D_{32}=\frac{6\bar{\rho}\tilde{Y}}{\rho_l\widetilde{\Sigma}} \tag{17}$$

The model was implemented using the OpenFOAM [13] library. The advantages of this library are that polyhedral mesh support and parallelism are intrinsically supported. The implementation details are described in Trask et al [15]

Results and Discussion

Experimental data

The data for model evaluation were obtained from Diesel sprays generated by a single-hole axisymmetric nozzle, using a high-pressure common rail system, with injection pressures ranging between 30 and 130 MPa. The sprays are injected into a quiescent vessel where back pressure is modified at constant room temperature, so that ambient densities from 10 to 40 kg/m^3 are obtained in a non-vaporizing environment.

Concerning nozzle geometry characteristics, summarized in Table 1, the orifice is convergent with 0.112 mm outlet diameter. This nozzle was hydro-eroded in order to round the edges of orifice inlet. Both geometric characteristics are aimed to prevent cavitation, as demonstrated by hydraulic characterization presented in [16].

D_o [mm]	*L/D [-]*	*r/D [-]*	*k-factor*
0.112	8.93	0.30	2.1

Table 1 Nozzle geometrical characteristics.

Although the Σ -Y approach was primarily aimed to describe the spray dense region in the vicinity of the nozzle orifice, it is very difficult to obtain experimental results in this region [17]. Validation in the present work is mainly based on two experimental sources, namely spray visualization and PDPA. It is true that especially the second technique provides information mainly in more diluted region. However, given the experimental difficulties previously mentioned in the near-nozzle region, a validation based on both techniques probably is also indicative of the accuracy of the model to describe the global spray behavior.

Spray macroscopic characteristics, namely penetration and cone angle, have been obtained by high-speed imaging. A detailed description of the experimental set-up and image acquisition methodology can be found in [18]. Regarding image processing, a validated methodology for segmentation was used [19]. The histogram distribution of digital level is obtained, a PDF is applied and a threshold value is statistically determined to obtain a binary image of the spray. Finally, connectivity algorithms are used to establish the spray contour, which makes geometrical measurements feasible.

An additional source of spray data are the droplet size and velocity measurements from [20], performed at different axial sections located from 25 to 50 mm to the orifice. As described in [21], a specific optimization of the PDPA system has been performed in order to improve measurements at those conditions.

Computational set-up

In order to simulate the Diesel sprays, a 2-D axisymmetric computational domain with 80 x 25 mm extent in the axial and radial spray directions is considered. The mesh is structured with non-uniform grid resolution. There are 10 cells along the orifice diameter, keeping an aspect ratio close to one in the near nozzle region, as depicted in Figure 1. A mesh size convergence study was performed in order to achieve grid independent results. The grid used in the calculations comprises 450 x 80 cells, with cell expansion ratio of 1.01 and 1.06 in axial and radial directions, respectively.

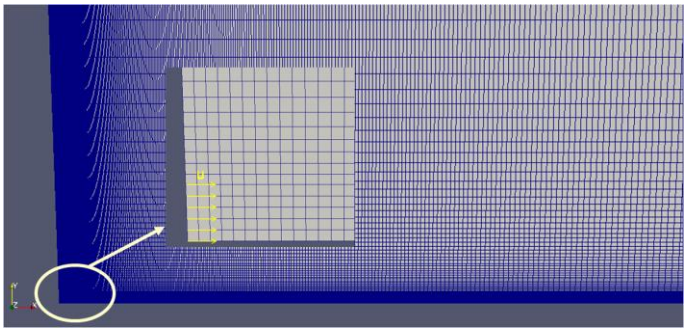

Figure 1 Computational grid.

A Gamma NVD scheme is used for discretization of divergence terms and a first order Euler scheme is applied for time derivative terms. The inlet velocity boundary condition is obtained from mass flow rate and momentum flux measurements, applying a constant radial profile of axial velocity and density at nozzle outlet. The turbulent intensity was set to 5% and the length scale as 10% of nozzle diameter.

Model set-up

One of the Σ-Y model's main assumptions is based on the calculation of spray dispersion from a variable density turbulent mixing flow, thus it is expected that turbulence modelling will have a strong effect on spray predictions. As previously described, a modified form of the k-ε model accounting for density variations is employed. Due to well known round jet spreading overprediction of k-ε type models [22], two different values for $C_{\varepsilon 1}$ constant were evaluated: the standard (1.44) and a corrected value for round jets (1.60). Though more refined expressions have been formulated for liquid turbulent flux closure [9], a gradient closure with Sc_t=0.9 is used for this term. Results presented by Lebas et al. [10][23] indicate that this formulation could be sufficiently accurate for high speed Diesel spray modelling.

Initial simulations were run for the 80 MPa injection pressure and 40 kg/m^3 ambient density conditions in order to evaluate the accuracy of the modelling approach. Results shown in Figure 2 indicate that good agreement of spray penetration, and also centreline velocity, is obtained when using the corrected $C_{\varepsilon 1}$ value. A noticeable underestimation is obtained when using the standard value. Moreover, the measured radial profiles of axial velocity can only be captured with the corrected $C_{\varepsilon 1}$, as depicted in Figure 3. It is also observed from this figure that self-similar velocities profiles are both obtained for measurements and calculations at those axial locations. These results indicate that both spray penetration and dispersion, which are related parameters, can be accurately predicted with the proposed model set-up. It is also noticeable that spray penetration is well predicted at initial stages but also far downstream of the primary atomization region.

The agreement between the model bulk velocity and the liquid measured one indicates very low slip between phases, at least for those conditions and measurement locations. This dynamic equilibrium also supports using a gradient closure for liquid turbulent flux, which provides very low slip velocities [9].

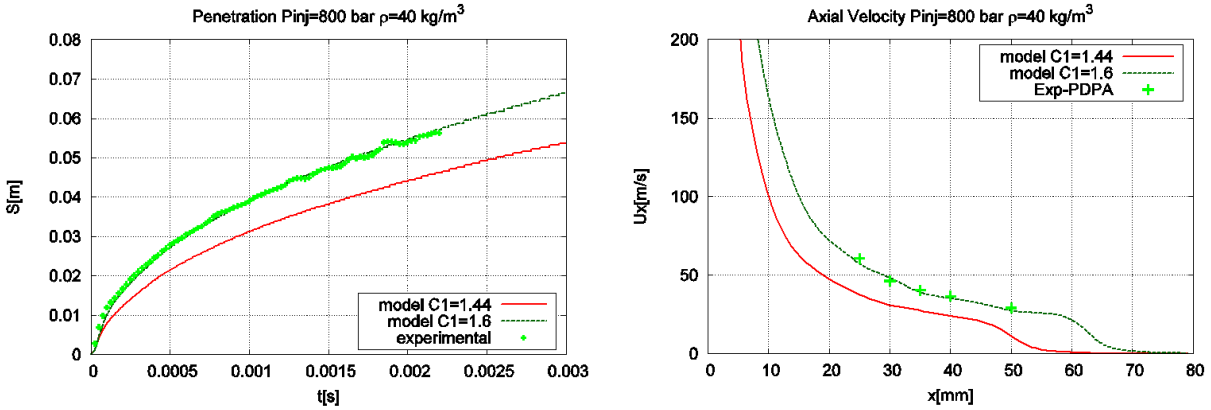

Figure 2 Spray tip penetration (left) and centerline axial velocity (right).

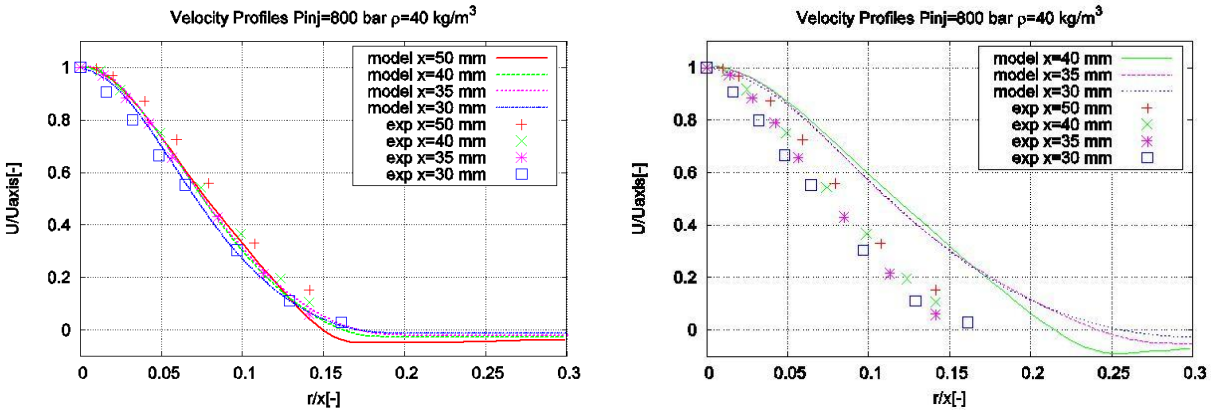

Figure 3 Measure and predicted normalized radial profiles of axial velocity with CFD model using $C_{\varepsilon 1}$=1.6 (left) and $C_{\varepsilon 1}$=1.44 (right)

The next step on model set-up, after spray large-scale flow, is focused on the small-scale atomization characteristics given by the interface surface density (Σ) and the droplet size derived from this variable. In this case, the Σ equation source and sink terms' constants correspond to the values proposed in [14], but α_2 is set to 2.5 in order to provide fair agreement with measured SMD levels. Figure 4 shows the predicted spray SMD contours, where SMD decreases just downstream the liquid core and after that increases progressively with axial distance. As depicted in Figure **5,** the measured SMD axial increase is smaller, especially for near-axis locations. The droplet average size increase for downstream locations, observed in this and other works [24][25] under non-evaporative conditions, is attributed to droplet coalescence. This behaviour is also obtained in calculations due to the predominance of surface density sink terms on Eq. (11), probably caused by the increased equilibrium radius r_{eq} with lower kinetic turbulent energy k.

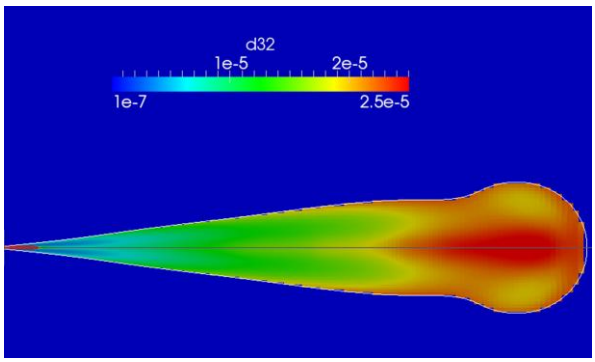

Figure 4 Calculated SMD contours.

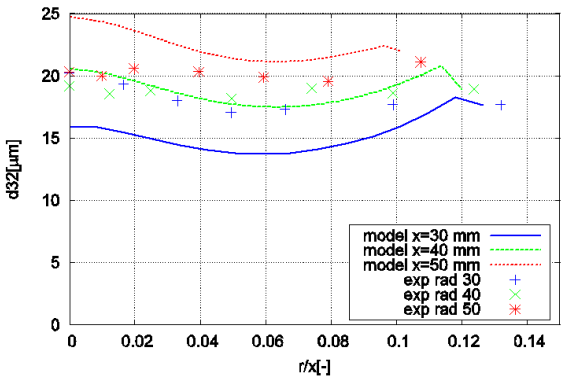

Figure 5 Measured and predicted SMD profiles.

Model evaluation

The model set-up defined in previous section was further assessed by simulating a series of experiments with different ambient and injection conditions. The range of validity of the model was evaluated by running cases with lower ambient density (25 and 10 kg/m^3) and increased (130 MPa) and decreased (30 MPa) injection pressures.

As shown in Figure 6, the accuracy of spray penetration predictions for high and intermediate ambient densities are similar, though some differences in centreline velocity results can be observed for ρ_a=25 kg/m^3 conditions. It is clearly depicted that spray penetration is under-predicted for the lower ambient density and also centerline velocities are lower than PDPA measurements. Velocity radial profiles from Figure 7 show reduced spray dispersion as ambient density decreases, but the narrower profiles for the lowest density case cannot be captured by the model.

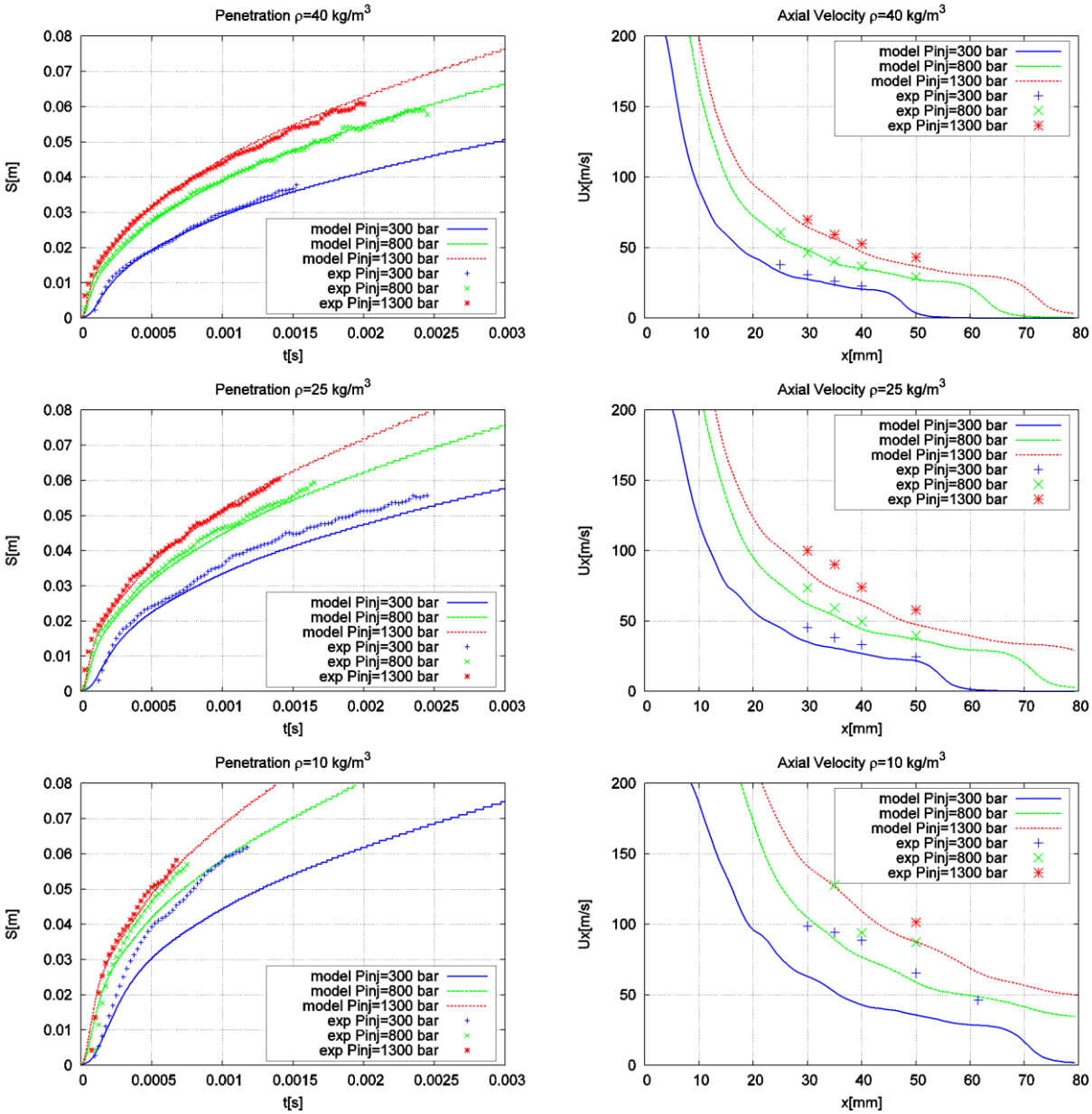

Figure 6 Spray penetration (left) and centerline axial velocity (right).

Higher injection pressure does not modify the accuracy of spray characteristics predictions, and even good agreement on tip penetration is obtained for the lowest ambient density condition. Fair predictions are still found for P_{inj}= 300 bar and ambient densities of 40 and 25 kg/m^3. Major discrepancies have been obtained for the lowest density and injection pressure condition. In this case both *Re* and ambient to fuel density ratio are decreased, so this may have an effect on spray atomization regime [26] and compromise the validity of the model assumptions. The slip between phases in these conditions is more significant and then the addition of a Lagrangian

tracking for sparse spray regimes [8] or a detailed model for the diffusion flux term closure, such as suggested in [9], could provide better predictions.

Figure 8 shows the predicted and measured SMD data at the same section as the velocity profiles from Figure 7. It is shown that SMD decreases with lower ambient density, probably due to lower coalescence after the primary atomization region [27]. This trend is captured by the model but the effect is overestimated. Concerning injection pressure effects, SMD increases for lower injection pressures, as expected, but also here the trend is overestimated compared to experimental data.

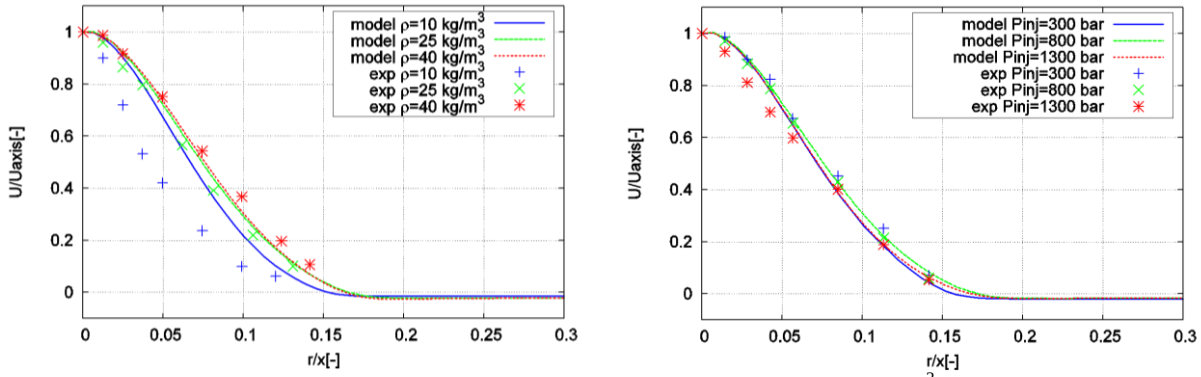

Figure 7 Axial velocity radial profiles for P_{inj}=800 bar (left) and ρ_a=40 kg/m^3 (right) at x=35 mm.

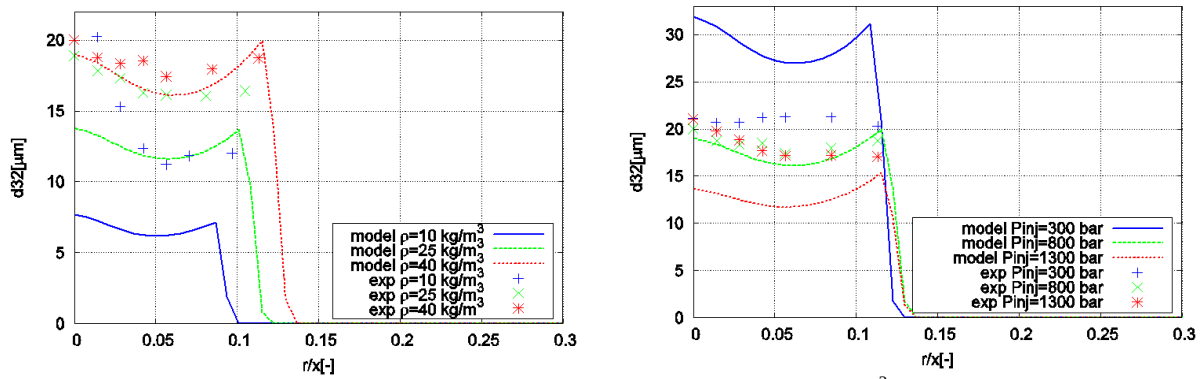

Figure 8 SMD radial profiles for P_{inj}=800 bar (left) and ρ_a=40 kg/m^3 (right) at x=35 mm.

Summary and Conclusions

A new, fully compressible implementation of the Σ-Y model has been applied to non-evaporating Diesel fuel injection. The test conditions, which cover a range of injection pressures and ambient gas densities, correspond to experiments run in a spray test rig. The calculations employed turbulence model settings that were previously suggested for round jets.

The model validation covered rates of tip penetration, velocity and SMD profiles at varying axial and radial locations. The tip penetration rates and velocity predictions were in very good agreement with the experimental data under medium and high ambient gas density conditions. When the ambient gas density was low, agreement was not as good, suggesting that the model assumptions are being violated. One likely explanation is that that the higher degree of slip between velocities at low ambient gas densities invalidates the assumption that the two-phases can be represented with a single velocity field. Under such conditions, transition to a Lagrangian formulation in the sparse region of the spray would be more appropriate. The model suggested by Beau et al. [9] may also improve the predictions in such low ambient density conditions.

The measured SMD were compared to the model predictions at several locations. For drop size predictions, the results of the model were only qualitatively correct. Though the model correctly predicted that drop size increased with high ambient gas density and decreased with injection pressure, the degree of variation was not correctly predicted.

The overall utility of the Σ-Y modelling approach is confirmed by the validation studies. The model is applicable to ambient gas density conditions that are normally present in Diesel engines, but would be less accurate for very early injection conditions, such as those found in highly premixed combustion strategies. The model is not yet capable of predicting drop sizes over the range of conditions studied. Given the significance of drop size prediction, this is a likely area for future research.

Acknowledgements

This work was partially funded by the Spanish Ministry of Education and Science in the frame of ENE2010-18542 project. The authors acknowledge support from the Army Research Office under grant number W911NF-08-1-0171.

References

[1] Dukowicz, J.K. *Journal of Computational Physics* 2:111-566 (1980)
[2] Abraham, J. *Transact. SAE* 106:141–155 (1997)
[3] Iyer, V., Abraham, J. *Combust. Sci. Technol.* 130:315-334 (1997)
[4] Abraham, J., Pickett, L.M. *Atomization and Sprays* 20:241-150 (2010)
[5] Som, S., Aggarwal, S.K. *Atomization and Sprays* 19:885–903 (2009)
[6] Vallet, A., Borghi, R., *C.R. Acad. Sci., Paris* 327:1015-1020 (1999)
[7] Vallet, A., Burluka, A.A., Borghi, R. *Atomization and Sprays* 11:619-642 (2001)
[8] Blokkeel, G., Barbeau, B., Borghi, R. *SAE Technical Paper* 2003-01-005 (2003)
[9] Beau, P.A., Funk, M., Lebas, R., Demoulin, F.X. *SAE Technical Paper* 2005-01-0220 (2005)
[10] Lebas, R., Menard, T., Beau, P.A., Berlemont, A., Demoulin, F.X. *Int. J. Multiphase Flow* 35:247-260 (2009)
[11] Desportes, A., Zellat, M., Desoutter, G., Liang, Y., Ravet, F. *THIESEL 2010 Conference on Thermo- and Fluid Dynamic Processes in Diesel Engines*, Valencia, Spain, September 11-14 (2010)
[12] Ning, W., Reitz, R.D., Diwakar, R., Lippert, A.M. *Atomization and Sprays* 19:727-739 (2009)
[13] Weller, H. G., Tabor, G., Jasak, H., Fureby, C. *Computers in Physics*, 12(6):620-631 (1998)
[14] Demoulin, F.X., Beau, P.A., Blokkeel, G., Mura, A., Borghi, R. *Atomization and Sprays* 17:315-345 (2007)
[15] Trask, N., Schmidt, D.P., Lightfoot, M.D.A., Danczyk, S.A. *J. Propulsion and Power*, in press (2012)
[16] Payri, R., Salvador, F. J., Gimeno, J.; Garcia, A. *Proc. of the IMechE, Part D* 226:133-144 (2012)
[17] Kastengren, A., Powell, C. F., Wang, Y.-J., Im, K.-S., and Wang, J., *21st Annual ILASS Conference*, Orlando, FL (2008).
[18] Payri, R., Salvador, F. J., Gimeno, J., Novella R. *Int. J. Heat And Fluid Flow* 32:273–284 (2011)
[19] Pastor, J.V., Arrègle, J., García, J.M., Zapata, L.D. *Appl. Opt.* 46:888-899 (2007)
[20] Payri, R., Tormos, B., Salvador, F. J., Araneo, L. *Fuel* 87:3176–3182 (2008)
[21] Araneo, L., Soare, V., Payri, R., Shakal, J. *J Phys: Conf Ser* 45:85–93 (2006)
[22] Pope, S. *AIAA* 16:279-281 (1978).
[23] Lebas, R, *PhD Thesis*, University of Rouen (2007)
[24] Araneo, L., Tropea, C., *SAE Technical Paper* 2000-01-2047 (2000)
[25] Baik, S., Blanchard, J.P., Corradini, M. *Atomization and Sprays* 13: 443-474 (2003)
[26] Reitz, R.D., Bracco, F.V. *The Encyclopedia of Fluid Mechanics* 10:233-249, Gulf Publishing (1986)
[27] Reitz, R.D., *Atomisation and Spray Technology* 3:309-337 (1987)